A Preliminary Study on Cyclic Behaviour of SFS Dowelled Connections in Glulam Frames

W. Dong & M. Li

University of Canterbury, Christchurch.

ABSTRACT

SFS self-drilling dowels are a special type of metal fasteners in timber construction which can go through relatively thin steel plates and timber members without pre-drilling. The application of SFS dowels makes wood-steel connection assembling more efficient and accurate. Due to tight fitting between holes and fasteners, initial slips in SFS dowelled connections are much smaller than that in conventional dowelled or bolted connections which have predrilled holes typically oversized with 1~2mm. So far, design of SFS dowelled connections in New Zealand mainly follows European practice and very limited experimental testing has been done to validate the SFS dowelled connection strength and stiffness with NZ Radiata Pine (RP). This paper presents a preliminary experimental study to investigate cyclic performance of SFS dowelled connections in RP glulam that are designed to connect diagonal braces with glulam beams and columns. Connection properties in terms of strength, stiffness, ductility and overstrength were derived from the force-displacement curves. The test results showed that the SFS connections performed well with high ductility. The design equations in Eurocode 5 also provided reasonably accurate ultimate strength, initial stiffness and ultimate stiffness predictions.

1 INTRODUCTION

Dowel-type connections with slotted-in steel plates provide multiple shear planes of fasteners and are one of the most efficient joint types for heavy timber structures (Figure 1). Common wood-steel-wood (WSW) dowelled or bolted connections require considerable manufacturing efforts including accurate drilling because fabrication tolerances can affect the performance of the connections (Mischler, et al.2000). However, to easily assemble dowels into steel plates and timber members, oversized holes are usually predrilled and often cause significant initial slip with reduced stiffness of the connections.

Paper 105

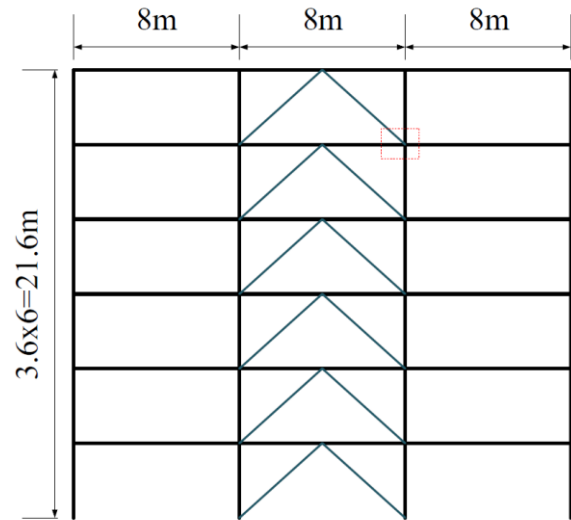Figure 1 Beatrice Tinsley Building at University of Canterbury

Figure 2 Building scenario for specimen design

SFS self-drilling dowels are a type of special fasteners which can go through timber members and relatively thin steel plates without pre-drilling. SFS dowels are commercially available in 7mm diameters and are considered as slender fasteners manufactured by high strength steel. As a proprietary product, very limited research on SFS dowels has been reported in literature. Mischler (2001) conducted axial monotonic tests of SFS dowelled connections in Norway spruce and observed high load-carrying capacity and ductile behaviour. Schreyer et al. (2004) conducted a series of dowelled connection tests in Parallel Strand Lumber (PSL) and compared test results between slender common dowels and SFS dowels and concluded that SFS dowels had overall comparable performance to common slender dowels with slightly improved monotonic stiffness and strength. Lau (2006) carried out compressive tests of SFS dowelled connections in Laminated Veneered Lumber (LVL) and found the connections performed better than bolted connections in terms of strength and stiffness. In New Zealand, SFS dowelled connections have been applied in timber construction and the design method mainly follows European Yield Models (EYMs) in Eurocode 5 (2004) since Timber Structures Standard NZS3603(1993) does not include this specific type of fasteners. Although generally treated as a slender dowel fastener, there is limited knowledge of the cyclic behaviour of SFS dowels with New Zealand RP glulam structure. Therefore, this study aims to understand the behaviour of the SFS dowelled connections under cyclic loading and the results are used to check against the prediction accuracy of the design equations.

2   EXPERIMENTAL PROGRAMME

2.1 Specimen design and material property

As shown in Figure 2, a six-storey glulam frame structure with K braces was used as the design scenario. The SFS dowelled connections were designed to connect the braces to the beams and columns. The layout of the connection specimen is shown in Figure 3. The component B-1 and C-1 were used to simulate the beam and column in the design building. GL10 RP glulam was used for B-1 and C-1 and the design properties are specified by NZS3603. The average moisture content of the glulam members was 14% and the average density was 478 kg/m³. The cross sections of B-1 and C-1 were 270mm x 225mm and 225mm x 225mm respectively. Two 8 mm wide slots were cut in B-1 and C-1 by a Computer Numerical Control (CNC) machine and two 6 mm thick steel gusset plates (S-1) were inserted into B-1 and C-1. One Φ60 mm hole was

drilled on each gusset plate to connect the actuator with a pinned connection. 6mm ring pads were welded around the hole to avoid any potential for local yielding around the holes. The steel plates had Grade 300 according to AS/NZS 3678 (2016).

Nine Φ7x173mm SFS dowels were used to fix S-1 to B-1 and C-1. The characteristic yield moment of SFS dowels is 31.93 kN·mm based on the supplier's document (Rothoblaas, 2017), which corresponds to a characteristic ultimate tensile strength of 675MPa according to Eurocode 5. Because B-1 and C-1 were 225mm thick, the SFS dowels were overdriven 20mm into the surface of B-1 and C-1. This centred the SFS dowels in the connection. The actuator applied the axial loading action from the braces in the design building and transferred the loads to the joints via the gusset plates.
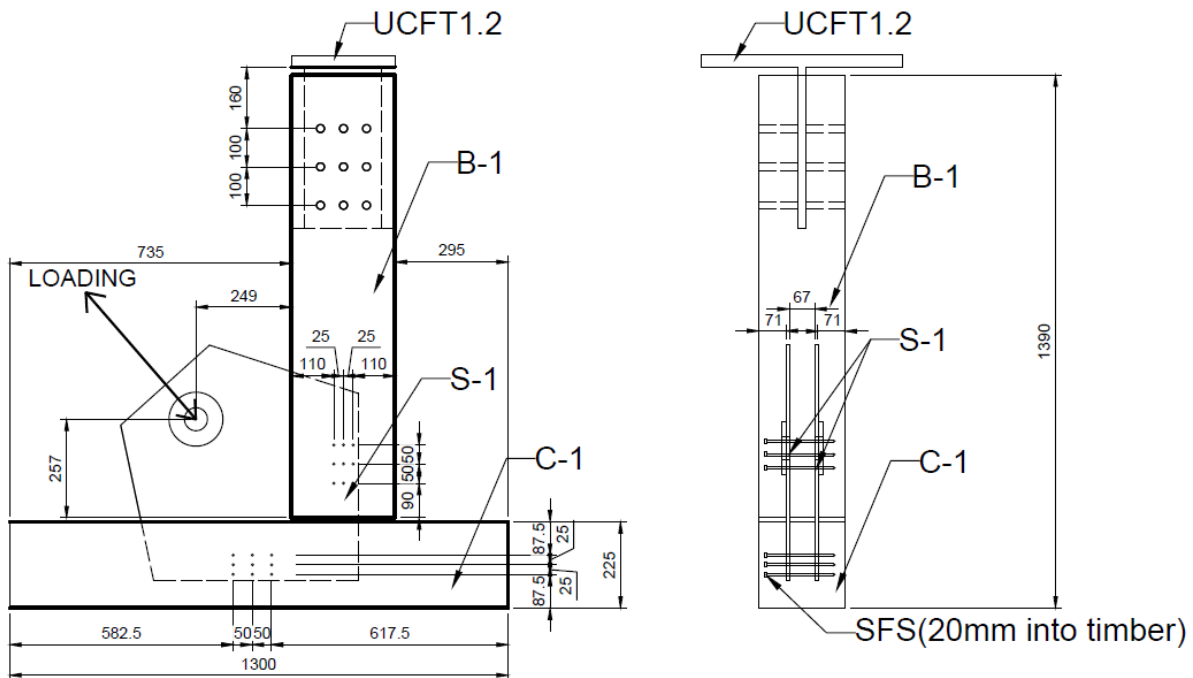

Figure 3 Specimen design

The test setup is shown in Figure 4 and three specimens (Specimen I, II and III) were tested. One side of the actuator was connected to the reaction wall and the other side was connected to the steel gusset plates of specimen. The beam part B-1 was restrained in tension and compression through UCFT1.2 fitting by Grade 300 dowels for specimen I or 4140 high strength dowels for specimen II and III. The UCFT1.2 was restrained by two Φ36 round steel bars in tension and two Φ70x6 steel tubes in compression. The column part C-1 was restrained by UCFT1.1 fittings. A 15mm gap was left under the column to minimize the amount of vertical load it would carry. In this way, C-1 would carry most of the horizontal force component from the actuator and B-1 would carry most of the vertical force component. This is consistent with the design assumption of the connection as a hinged one.

2.2 Loading protocol

The cyclic tests followed the loading protocol in EN12512 (2001) and the loading protocol is shown in Figure 5. The yield displacement used to define the loading protocol was assumed as 1.8mm conservatively according to the monotonic test results by Schreyer (2002).
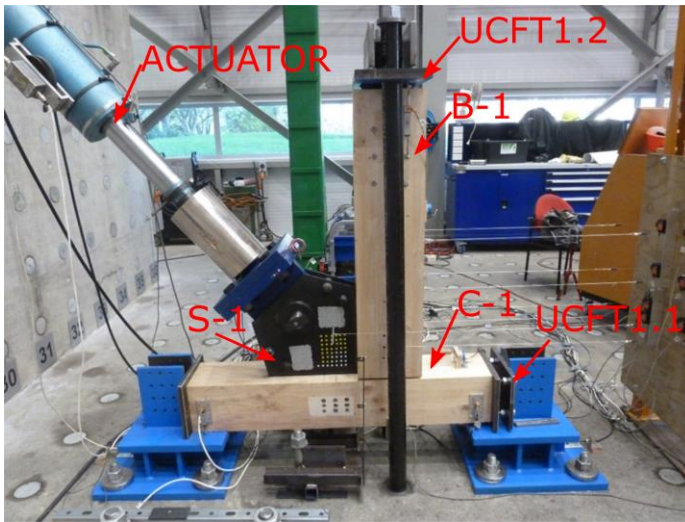
Paper 105 –Cyclic behaviour of SFS Dowelled Connections in Glulam Frames
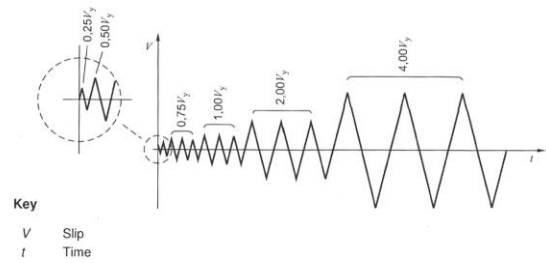
Figure 4 Test setup

Figure 5 Loading protocol from EN12512 (2001)

2.3 Instrumentation by potentiometers and PTV technique

Instruments were installed to measure the displacements of members and the connections. In addition to this, Particle tracking velocimetry (PTV) technique was also applied to capture the displacement and/or rotations. PTV is a quantitative field measuring technique originally designed to track individual particles in fluid flows. In timber connection testing, PTV is able to capture crack growth of exposed timber surfaces in dowelled connections and also compute the resulting displacement field in the connection area (Ottenhaus, et al. 2018). Figure 6 shows the small particles (white and yellow dots) painted on the surface of C-1 and S-1 during the tests. Potentiometers were also installed for the comparison. Because the SFS dowelled connection area in B-1 was covered by the steel tubes as part of the reaction frame, the movement could only be captured by potentiometers. Since the gusset plates were inserted into the timber, the displacement of the part covered by timber could only be tracked by the movement of particles outside the timber with PTV. Therefore, in this testing, the potentiometers and PTV complemented each other and helped to extract as much information as possible from the tests.
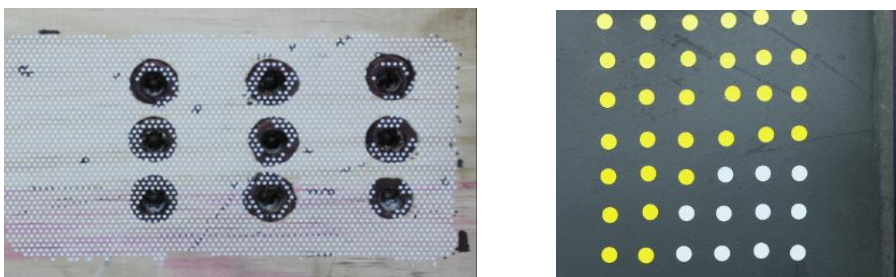

Figure 6 Particles on the timber and gusset plates

3   EXPERIMENTAL RESULTS

3.1 Failure mode

The tests were stopped when the strength decreased to 80% of the maximum load, which provides required data to derive connection strength, stiffness and ductility. During the tests, rotations of B-1, C-1 and S-1 were observed but no cracks in the glulam components were observed. To investigate the failure mechanism in the joints, specimens were cut open, as shown in Figure 7. Significant bending yielding deformation of the SFS dowels and timber embedment crushing (Figure 7a) were observed in the joint connecting the gusset

Paper 105 –Cyclic behaviour of SFS Dowelled Connections in Glulam Frames

plates with the C-1 member. Fastener bending yielding and wood embedment crushing is typically observed in ductile dowelled connections. Under the cyclic loading, low-cycle fatigue failure of the dowels were also observed, as shown in Figure 7b. However, no significant residual bending deformation of SFS dowels and timber crushing were observed in the joint in B-1, as shown in Figure 7c. It indicated that C-1 carried much higher load than B-1 and the joint in C-1 experienced more nonlinear deformation and dissipated more energy. One reasons was that UCFT1.1 fitting provided more restraints to restrict the horizontal and rotational movement of C-1 than the UCFT1.2 fitting on B-1. Another reason might be due to the loading eccentricity from the gusset plates S-1. Therefore, the failure of this connection was due to the failure of SFS dowels in C-1 because of uneven load distribution between the joints in C-1 and B-1.
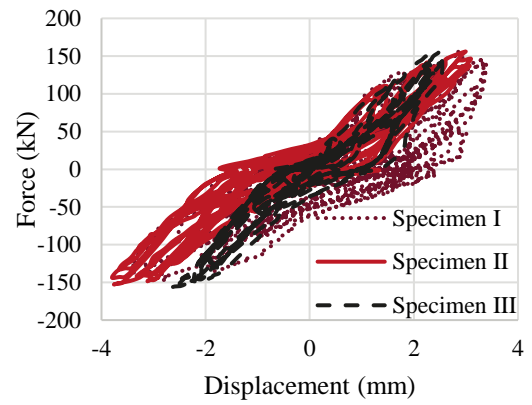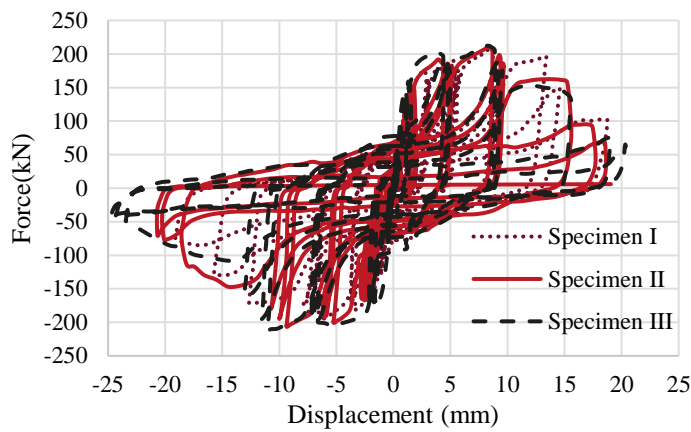

a) Timber embedment failure   *b) SFS dowel fatigue rupture in C-1*   *c) SFS dowels in B-1*

Figure 7 The cut-open specimen after failure

3.2 Connection properties

Figure 7a also shows that the load carried by C-1 was oriented at angle about 20° with respect to the horizontal direction. It was consistent with the trajectory recorded from PTV. B-1 was restrained only in the vertical direction, thus it only carried forces vertically. Thus, the total applied load by the actuator can be distributed to C-1 and B-1 according to the fastener deformation angle and the restraint conditions of C-1 and B-1. Figure 8a and 8b show the force-displacement hysteresis curves of the joints in C-1 and B-1, respectively. Based on Figure 8b, it can be seen that the joint in B-1 had much smaller slips and the load level was much lower than the joint in C-1. This is consistent with the negligible damage observed, as shown in Figure 7c. Figure 9 shows the envelop curves of Figure 8a of the joint in C-1. The average of the positive and negative curves was used to derive the connection properties. Table 1 lists the summary of the properties of the joint in C-1 of the three specimens in terms of yield force F_y, maximum strength F_{max}, ultimate strength F_u, yield displacement Δ_y, ultimate displacement Δ_u, initial stiffness K and ductility μ. The definitions of yield displacement Δ_y and ultimate displacement Δ_u are followed EN12512. The ductility factor μ is defined as:

$$\mu = \frac{V_u}{V_y} \tag{1}$$

Paper 105 –Cyclic behaviour of SFS Dowelled Connections in Glulam Frames

a) C-1 connection for three specimens

b) B-1 connection for specimen III

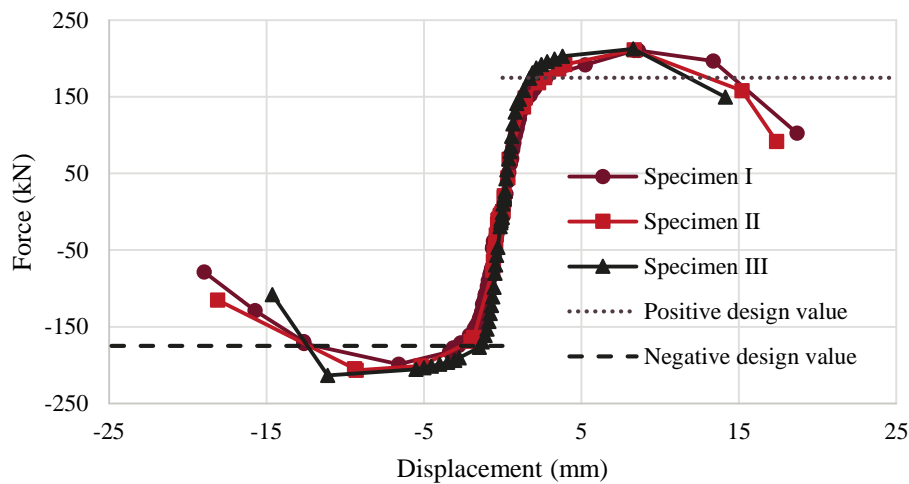*Figure 8 Force-displacement curve of the specimens*

Figure 9 Envelope force-displacement cycle curves

Table 1 The specimens test results

Specimen No.	Specimen I	Specimen II	Specimen III	Average
F_y (kN)	147.5	154.3	158.0	153.3
F_{max} (kN)	204.5	209.0	212.9	208.8
F_u (kN)	163.6	167.2	170.3	167.0
Δ_y (mm)	1.3	1.6	0.9	1.31
Δ_u (mm)	14.3	13.5	12.4	13.4
K (kN/mm)	119.5	90.8	169.5	126.6
μ	10.8	8.3	13.1	10.8

Paper 105 –Cyclic behaviour of SFS Dowelled Connections in Glulam Frames

3.2.1 Stiffness degradation

Stiffness degradation is an important parameter to estimate the performance of the connections under cyclic loading. The secant stiffness of each loading cycle was calculated by Equation 2:

$$K_i = \frac{|F_{ip}| + |F_{in}|}{|\Delta_{ip}| + |\Delta_{in}|} \qquad (2)$$

where F_{ip}= the maximum positive load of cycle i; F_{in}= the maximum negative load of cycle i; Δ_{ip}= the displacement corresponding to F_{ip}; Δ_{in}= the displacement corresponding to F_{in}

Figure 10 shows the decrease of the stiffness with the increase of the displacement. As illustrated, the initial stiffness was high due to the tight fit of the SFS dowels. It decreased to half of the initial stiffness at around 3mm because the wood embedment started to crush and the fasteners started to yield. However, From Figure 8b, the joint in B-1 did not show much yielding and stiffness degradation after 3mm's displacement. The reason is that the displacement contains the fastener slip in UCFT1.2 fitting which has oversized holes as well. Also the displacement of SFS dowel group was recorded by potentiometers which included horizontal displacement component as well.

3.2.2 Energy dissipation

The energy dissipation capacity of connection is critical for timber construction under severe earthquakes and it plays a key role for the structure to sustain the loads and prevent collapse. Figure 11 shows the accumulative energy dissipation curve by evaluating the enclosed area of the force-displacement hysteretic loops in Figure 8a. The hysteretic energy dissipation was small during the first eleven loading cycles with small displacement magnitude, indicating that the SFS dowels behaved approximately elastically up to a maximum deformation of 1.85mm. After that, the SFS dowels started to yield, the energy dissipation increased significantly.
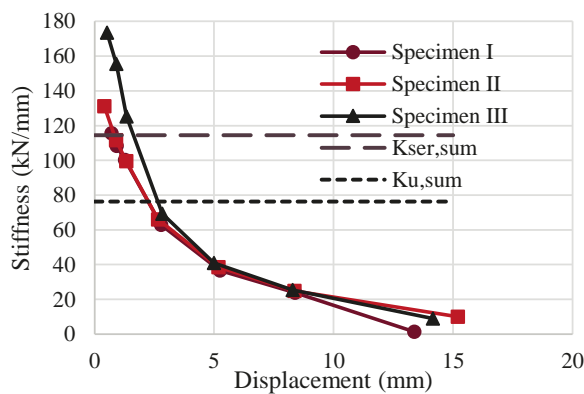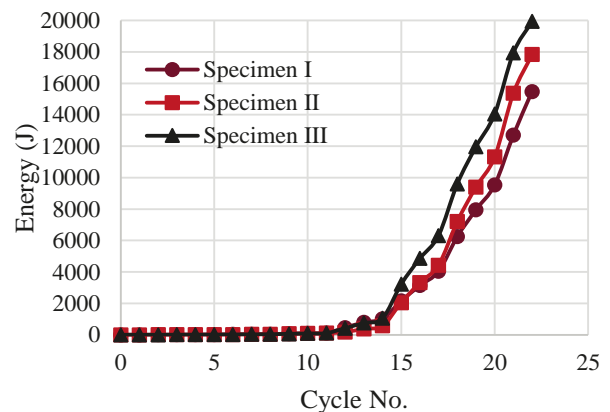

Figure 10 Stiffness degradation

Figure 11 Energy dissipation curve

3.3 Design predictions vs. test results

The strength and stiffness of the connections can be predicted by Equation 3 to Equation 12 according to the Eurocode 5. For each SFS dowel, four shear planes are considered.

$$n_{ef} = \min\left\{ n, n^{0.9} \sqrt[4]{\frac{a_1}{13d}} \right\} \qquad (3)$$

Paper 105 –Cyclic behaviour of SFS Dowelled Connections in Glulam Frames

$$F_{v,Rk} = \min \begin{cases} f_{h,\alpha,k}t_1 d \\ f_{h,\alpha,k}t_1 d \left[\sqrt{2 + \frac{4M_{y,Rk}}{f_{h,1,k}dt_1^2}} - 1 \right] + \frac{F_{ax,Rk}}{4} \\ 2.3\sqrt{M_{y,Rk}f_{h,\alpha,k}d} + \frac{F_{ax,Rk}}{4} \end{cases} \tag{4}$$

$$f_{h,0,k} = 0.082 \times (1 - 0.01d)\rho_k \tag{5}$$

$$f_{h,\alpha,k} = \frac{f_{h,0,k}}{k_{90}\sin^2\alpha + \cos^2\alpha} \tag{6}$$

$$F_{pred} = n_{ef} \cdot n_2 F_{v,Rk} \tag{7}$$

$$k_{90} = 1.35 + 0.015d \tag{8}$$

$$K_{ser} = \rho_m^{1.5}d/23 \tag{9}$$

$$K_u = \frac{2}{3}K_{ser} \tag{10}$$

$$K_{ser,sum} = n \cdot n_2 K_{ser} \tag{11}$$

$$K_{u,sum} = \frac{2}{3}K_{ser,sum} \tag{12}$$

Where, n= the number of dowels in the row, n_{ef}= effective number of dowels for one row, a_1= the spacing between dowels in the grain direction (mm), d= the dowel diameter (mm), $F_{v,Rk}$ = load-carrying capacity for dowels per shear plane per fastener (N), α= the angle of the load to the grain (°), ρ_k= the characteristic timber density (kg/m³), $f_{h,0,k}$= the characteristic embedment strength parallel to grain (N/mm²), $f_{h,\alpha,k}$= the characteristic embedment strength at an angle of α to the grain(N/mm²), t_1 is the smaller of the thickness of the timber side member (mm), $M_{y,Rk}$= the characteristic fastener yield moment (N·mm), $F_{ax,Rk}$= the characteristic withdrawal capacity of the fastener (N), n_2= the number of rows, K_{ser}= slip modulus per shear plane per fastener under service load (N/mm), ρ_m= the mean timber density (kg/m³), K_u= slip modulus per shear plane per fastener under ultimate limit state (N/mm), $K_{ser,sum}$= slip modulus of the connection under service load (N/mm), $K_{u,sum}$= slip modulus of the connection under ultimate limit state (N/mm),

The $F_{ax,Rk}$ is considered as zero in these connections. The characteristic density is not offered because the low number of specimens was not statistically significant. The minimum density of all specimens was assumed as characteristic density to calculate $f_{h,0,k}$. Franke and Quenneville (2010) found that Eurocode 5 overestimated $f_{h,0,k}$ for small diameter dowels. Therefore, this assumption will produce a relatively conservative strength prediction. The parameters for calculating the strength and stiffness are listed in Table 2.

To ensure a structural system can mobilise its ductile potential, design demand for the brittle components and failure modes needs to be increased by applying an overstrength factor γ_Rd to the calculated ductile component strength as shown in Equation 13 (Ottenhaus, et al. 2017).

$$F_{Dd} \cdot \gamma_{Rd} \leq \min\{F_{Bd}, F_{member,d}\} \tag{13}$$

Where, F_{Dd}= design capacity of ductile components, F_{Bd}= design capacity of brittle components, $F_{member,d}$= design capacity of elastic members.

Design codes specify the relationship of the design capacity and the characteristic value by γ_M, which depends on different materials. By assume that all components have the same γ_M, the characteristic values for each dowel group will be used to estimate the overstrength value. The results are listed in Table 3 and F_{pred} is the predicted characteristic load capacity based on Eurocode 5.

Figure 9 and Figure 10 shows the predicted strength and stiffness. From Figure 9-10, the predict strength is close to the maximum strength of the connection with an average overstrength value of 1.19. At the same time, the stiffness is around 65.9kN/mm, which is close to the $K_{u,sum}$. The F_{pred} and $K_{u,sum}$ can be considered as a reasonably prediction for ultimate strength and stiffness. In addition to that, $K_{ser,sum}$ is close to initial stiffness K and can be used as a prediction of K.

Table 2 Parameters in Eurocode 5

n	n_{ef}	a_1	d	α	ρ_k	ρ_m	$f_{h,0,k}$	$f_{h,\alpha,k}$	t_1	$M_{v,Rk}$	$F_{v,Rk}$	K_{ser}	K_u
3	2.3	50	7	20	463	478	34.3	32.6	71	31930	6296	3180	2120

Table 3 Prediction based on Eurocode 5 and the overstrength value

	Specimen I	**Specimen II**	**Specimen III**	**Average**
F_y (kN)	147.5	154.3	158.0	153.3
F_{max}(kN)	204.5	209.0	212.9	208.8
F_{pred}(kN)		174.8		
γ_M (F_{max}/F_{pred})	1.17	1.22	1.23	1.19
K(kN/mm)	119.5	90.8	169.5	126.6
$K_{ser,sum}$(kN/mm)		114.5		
$K_{u,sum}$		76.3		

3.4 Potentiometers measurements vs. PTV

In general, the displacement measurements between potentiometers and PTV agreed very well. As an example, Figure 12 shows the recorded time history of vertical displacement relative to the ground at centre of the SFS dowel group in C-1. Overall, the potentiometer measurement was slightly higher than the PTV measurement. The reason might be that the potentiometer actually recorded the total displacement between two measuring points, including both horizontal and vertical component. However, the PTV only recorded the vertical component. Therefore, slight rotation of the connection in this test led to the slight difference between the potentiometer measurement and the PTV measurement.
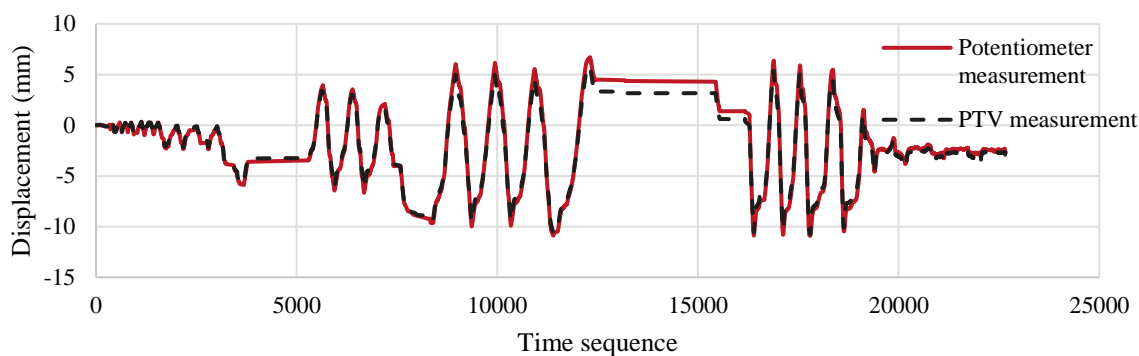
Paper 105 –Cyclic behaviour of SFS Dowelled Connections in Glulam Frames

Figure 12 The comparison between potentiometers and PTV

4 CONCLUSIONS

This study presents a preliminary experimental study on cyclic performance of SFS dowelled connections in GL10 grade glulam. The following conclusions can be drawn:

- The SFS dowel connections performed well with high strength, initial stiffness, ductility and good energy dissipation capacity based on the results of three connection specimens.
- The predicted equation based on Eurocode 5 provided reasonably good predictions of the connection maximum strength and initial stiffness.
- The PTV measurement matches the potentiometer measurement well and they can complement each other during the tests.

5 ACKNOWLEDGEMENTS

6 REFERENCES

BSI. (2001). BS EN 12512: 2001: Timber structures–Test methods–Cyclic testing of joints made with mechanical fasteners.

CEN. EN 1995-1-1: Eurocode 5: design of timber structures – Part 1–1: General – Common rules and rules for buildings, CEN, Brussels, Belgium; 2004.

Franke, S., & Quenneville, P. (2010). *Embedding behaviour of LVL and radiata pine lumber.* Paper presented at the Proceedings of 11th World Conference on Timber Engineering, Italy.

Lau, P. H. (2006). *Fire Resistance of Connections in Laminated Veneer Lumber (LVL).* University of Canterbury. Retrieved from http://hdl.handle.net/10092/1089

Mischler, A. (2001). *Multiple Shear Steel-to-Timber Connections with Self-Drilling Dowels.* Paper presented at the IABSE Symposium Report.

Mischler, A., Prion, H., & Lam, F. (2000). *Load-carrying behaviour of steel-to-timber dowel connections.* Paper presented at the Proceedings of world conference of timber engineering, British Columbia, Canada.

Ottenhaus, L.-M., Li, M., Smith, T., & Quenneville, P. (2018). Overstrength of dowelled CLT connections under monotonic and cyclic loading. *Bulletin of Earthquake Engineering, 16*(2), 753-773.

Ottenhaus, L., Li, M., & Nokes, R. (2018). *Application of Particle Tracking in Large Scale Timber Connection Testing*. Paper presented at the World Conference on Timber Engineering, Seoul, Republic of Korea.

Paper 105 –Cyclic behaviour of SFS Dowelled Connections in Glulam Frames

Rothoblaas. (2017). *WS Technical data sheets* Retrieved from
https://www.rothoblaas.com/products/fastening/brackets-and-plates/pins-bolts-metric/ws#documents

SA, & SNZ. (2016). AS/NZS 3678:2016 Structural steel - Hot-rolled plates, floorplates and slabs: Standards Australia & New Zealand.

Schreyer, A. C. (2002). *Monotonic and cyclic behaviour of slender dowell-type fasteners in wood-steel-wood-connections.* University of British Columbia.

Schreyer, A. C., Lam, F., & Prion, H. G. (2004). Comparison of Slender Dowel-type fasteners for slotted-in steel plate connections under monotonic and cyclic loading. *Proc. 8th WCTE Lahti, 2*, 107-112.

SNZ. (1993). NZS 3603:1993 Timber Structures Standard. Wellington: Standards New Zealand.

Paper 105 –Cyclic behaviour of SFS Dowelled Connections in Glulam Frames